Vibronic Interaction in Metalloporphyrin π-Anion Radicals

Kazunari Yoshizawa,*,† Tomonori Nakayama,† Takashi Kamachi,† and Pawel M. Kozlowski*,‡

Institute for Materials Chemistry and Engineering, Kyushu University, Fukuoka 812-8581, Japan, and Department of Chemistry, University of Louisville, Kentucky 40292

Received: October 10, 2006; In Final Form: December 2, 2006

The vibronic (vibrational−electronic) interactions in the π-anion radicals of the metalloporphyrins (M=Cr, Mn, Fe, Co, Ni, Cu, and Zn), which show delocalized D_{4h} structures in the neutral states, are discussed using B3LYP density-functional-theory calculations. The B_{1g} and B_{2g} modes of vibration can remove the degenerate ^2E_g state of the π-anion radicals in the D_{4h} symmetric structures to lead to rectangular and diamond D_{2h} distortions, respectively. Calculated vibronic coupling constants demonstrate that the B_{1g} modes of vibration better couple with the degenerate electronic state, leading to the rectangular D_{2h} distortion. In particular, the B_{1g} modes of ν_{10} and ν_{11}, which have dominant contributions from C_α−C_m and C_β−C_β stretching, give large vibronic coupling constants in the π-anion radicals. The vibronic coupling constant can be viewed as the Jahn−Teller distortion force, and therefore these C−C stretching B_{1g} modes will play a central role in the Jahn−Teller effect of the π-anion radicals of the metalloporphyrins.

Introduction

The π-cation and -anion radicals of metalloporphyrins play essential roles in a lot of biological processes. For example, the radical species produced by the one-electron oxidation and reduction of the porhyrin ring are transient intermediates that function in the important reaction pathway of photosynthesis.[1−3] Metalloporphyrins have two nearly degenerate highest-occupied molecular orbitals (HOMOs) of a_{1u} and a_{2u} and two-fold degenerate lowest-unoccupied molecular orbitals (LUMOs) of e_g in the D_{4h} molecular structure,[4] as shown in Figure 1. These delocalized frontier orbitals that belong to the π orbitals of the porphyrin ring provide essential contributions to the absorption and emission spectra of metalloporphyrins. On the other hand, the central metal ions have minor perturbation effects to the π-electron system of the porphyrin ring.

The purpose of this work is to investigate the Jahn−Teller (JT) effect of the π-anion radicals of metalloporphyrins in terms of vibronic (vibrational−electronic) coupling constants, which describe a measure of interaction between electronic states and nuclear displacements from the initial configuration.[5] The problem of how electrons determine molecular configurations can be formulated and solved approximately by means of vibronic coupling constants. The vibronic interactions in metalloporphyrins and their role in structural distortion and spectroscopy were theoretically discussed in a series of papers by Bersuker and Stavrov.[6] Here we turn our attention to the vibronic coupling constants for certain modes of vibration in the π-anion radicals of metalloporphyrins.

Upon one-electron reduction, the e_g LUMOs are singly occupied. The resultant ^2E_g state of the π-anion radicals of metalloporphyrins is subject to a structural distortion from D_{4h} to D_{2h} as a result of the JT effect,[7,8] whereas the π-cation radicals distort their structures from D_{4h} to C_{4h} owing to the pseudo-JT effect.[7−11] The JT effect of the ^2E_g state of various porphyrin π-anion radicals was extensively characterized by means of spectroscopic measurements such as electron spin resonance.[12] Resonance Raman spectroscopy is also a useful probe of the porphyrin ring; it has been extensively applied to investigate the electronic and structural properties of metalloporphyrin species including the π-cation and anion radicals.[13−16] Bocian and co-workers[17] and Spiro and co-workers[18] observed π-anion radicals of metalloporphyrins generated electrochemically using resonance Raman spectroscopy and demonstrated that a static JT distortion from D_{4h} to D_{2h} is induced predominantly by the B_{1g} modes of vibration.

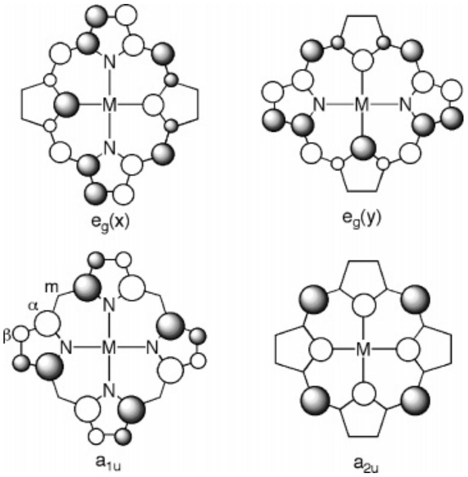

Figure 1. Illustration of the nearly degenerate a_{1u} and a_{2u} HOMOs and the degenerate e_g LUMOs.

In this study we have systematically calculated the vibronic coupling constants for the π-anion radicals of the metalloporphyrins incorporating Cr, Mn, Fe, Co, Ni, Cu, and Zn using density functional theory (DFT) to look at which mode of vibration plays a principal role in the JT distortion. First, fundamental aspects on the vibronic interaction and the JT effect in the metalloporphyrin systems are overviewed. Since the vibronic coupling in discrete molecules can be viewed as the interaction between frontier molecular orbitals and specific

---

* Corresponding authors. E-mails: kazunari@ms.ifoc.kyushu-u.ac.jp (K.Y.); pawel@louisville.edu (P.M.K.).

† Kyushu University.

‡ Visiting professor at Kyushu University from University of Louisville.

10.1021/jp0666479 CCC: \$37.00

TABLE 1: Spin Multiplicities of the Neutral and Anionic Ground States of the Metalloporphyrins

	Cr	Mn	Fe	Co	Ni	Cu	Zn
neutral	$^5B_{2g}$	$^6A_{2g}$	$^3B_{2g}$	$^2A_{1g}$	$^1A_{1g}$	$^2B_{1g}$	$^1A_{1g}$
anionic	$^4B_{1g}$	$^5B_{2g}$	$^4B_{2g}$	$^3B_{1g}$	$^2B_{1g}$	$^3B_{1g}$	$^2B_{1g}$

molecular vibrations, we develop our discussion in terms of molecular orbital interactions. Second, numerical results of the vibronic coupling constants are presented to add new insight into the JT-active vibrational modes of the π-anion radicals of the metalloporphyrins. We look at how specific modes of vibration have interaction with the degenerate electronic state and would lead to the JT distortion from D_{4h} to D_{2h} through the B_{1g} modes of vibration.

Vibronic Interaction in Metalloporphyrin π-Anion Radicals

The spin multiplicities of the neutral and anionic states of the metalloporphyrins are listed in Table 1. In the neutral states, all the unpaired electrons reside on the d-block orbitals and the two nearly degenerate π HOMO and HOMO-1 of a_{1u} and a_{2u} symmetry of the porphyrin ring. In the anionic states, one electron is not added to the open d-block orbitals but to the degenerate e_g LUMOs that belong to the π orbitals of the porphyrin ring. This electronic feature in the metalloporphyrins can be explained in terms of Gouterman's four-orbital model.[4] The addition of one electron to the neutral metalloporphyrins leads to the formation of the π-anion radicals, in which the degenerate e_g LUMOs are occupied by a single electron. This ^2E_g state is unstable, and therefore a JT distortion will take place to remove this electronic degeneracy. This is a typical case for twofold degenerate E states for systems containing symmetry axis of orders multiple by 4.[5] The direct product of the E_g electronic state of the π-anion radicals can be reduced as follows:

$$E_g \times E_g = A_{1g} + A_{2g} + B_{1g} + B_{2g} \tag{1}$$

The B_{1g} and B_{2g} modes of vibration can lift the degenerate ^2E_g state of the π-anion radicals in principle, whereas the A_{1g} and A_{2g} modes of vibration retain the fourfold axis of symmetry, so they cannot couple with the degenerate electronic state. The B_{1g} modes of vibration change the D_{4h} structure of the porphyrin ring to a rectangular structure while the B_{2g} modes induce a diamond distortion. Although both the B_{1g} and B_{2g} modes of vibration lead to symmetry lowering from D_{4h} to D_{2h}, only the B_{1g} modes are effectively JT active.[17,18] This is a direct consequence of the interaction between the e_g LUMOs and these molecular vibrational modes, as discussed below.

Figure 2 shows a schematic representation of A_{1g}, A_{2g}, B_{1g}, and B_{2g} modes of vibration, in which only the nuclear motions of the four nitrogen atoms are shown for simplicity. Let us look at an interesting relationship between the degenerate e_g LUMOs in Figure 1 and the B_{1g} and B_{2g} modes of vibration. When the porphyrin ring is distorted by the nuclear motion along the B_{1g} mode, one component of the degenerate e_g LUMOs ($e_g(x)$) is stabilized in energy while the other component ($e_g(y)$) is destabilized, due to the antibonding interaction in each pair of two opposite nitrogen atoms. As a result, the orbital degeneracy is effectively removed by the nuclear motion along the B_{1g} mode. We expect that although there are a large number of JT active modes, a few specific B_{1g} modes should have large vibronic coupling constants in the π-anion radicals. The purpose of this study is to find such JT active modes by computing vibronic coupling constants. On the other hand, the degenerate e_g LUMOs are unlikely to be effectively split by the nuclear motion along the B_{2g} mode because there is no direct orbital interaction between the neighboring nitrogen atoms in the e_g LUMOs. Thus, the B_{2g} modes will not have significant interactions with the ^2E_g state of the π-anion radicals in comparison with the B_{1g} modes. This qualitative orbital interaction analysis is useful in considering numerical results of the vibronic interaction.

Method of Calculation

We carried out all the calculations in this work using the hybrid Becke−Lee−Yang−Parr (B3LYP) functional[19−21] and the 6-31G(d) basis set (5d components)[22] implemented in the Gaussian03 program.[23] This level of theory is appropriate for structural analyses, molecular vibrations, and electronic properties of metalloporphyrins.[9−11] To elucidate electronic properties of the π-anion radicals, a series of metalloporphyrins incorporating a variety of transition metals (Cr, Mn, Fe, Co, Ni, Cu, and Zn) without peripheral substituents was analyzed. For each metalloporphyrin under consideration, the structure has been fully optimized in the neutral charge state assuming D_{4h} symmetry, and the resulting electronic configuration was verified to correspond to a stable electronic minimum by performing an analysis of the stability of the wave function. In each optimized geometry, harmonic frequencies were calculated to look at the optimized structure to correspond to a stable minimum. In all cases the stable minimum was confirmed except for Ni porphyrin. The optimized D_{4h} structure of Ni porphyrin in the neutral state has a small imaginary vibrational mode of 30.0 cm^{-1}. This imaginary mode is assigned to the so-called porphyrin ruffling motion that leads the planar porphyrin structure to a twisted nonplanar one.[24] Strictly speaking, the D_{4h} structure is not stable in energy in neutral Ni porphyrin; in fact, this structure is the transition state that connects equivalent two ruffled structures. This result is fully consistent with a resonance Raman spectroscopic analysis for Ni octaethylporphyrin in solution.[25] However, in this work we restrict our discussion to in-plane motions of the porphyrin ring from D_{4h} to D_{2h}, according to the JT effect. We can reasonably neglect this small imaginary mode of Ni porphyrin in the vibronic coupling analysis because the out-of-plane ruffling motion is expected not to couple with the in-plane JT distortion.

A series of metalloporphyrin π-anion radicals were generated by adding one electron to the optimized structures for the neutral species. In this one-electron reduced state, the D_{4h} structures are unstable and distorted to D_{2h} structures in order to remove the electronic degeneracy of the ^2E_g state, as mentioned earlier. The derivatives of the total energy of the π-anion radicals were computed by slightly distorting the optimized D_{4h} structures along each B_{1g} or B_{2g} vibrational normal coordinate. The quantity obtained from the gradient of the total energy curve at the original D_{4h} structure corresponds to the vibronic coupling constant, which characterizes the measure of interaction between the electronic state and nuclear displacements. This quantity can be viewed as the JT distortion force that will lower the molecular symmetry.[5] Therefore, one can predict which mode of vibration plays a major role in the structural change from D_{4h} to D_{2h} symmetry. The dimensionless vibronic coupling constant for the mth B_{1g} vibrational mode of the π-anion radicals is defined as follows:

$$g_{B1g,m} = \frac{1}{2\hbar\omega_m}\left\langle E_g \left| \left(\frac{\partial V}{\partial q_{B1g,m}}\right)_0 \right| E_g \right\rangle, \quad q_{B1g,m} = \left(\frac{\omega_m}{\hbar}\right)^{1/2} Q_{B1g,m} \tag{2}$$

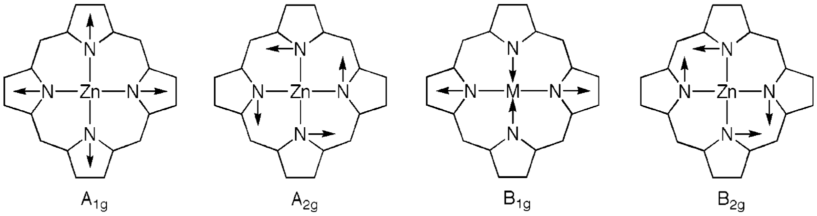

Figure 2. Schematic representation of A_{1g}, A_{2g}, B_{1g}, and B_{2g} modes of vibration.

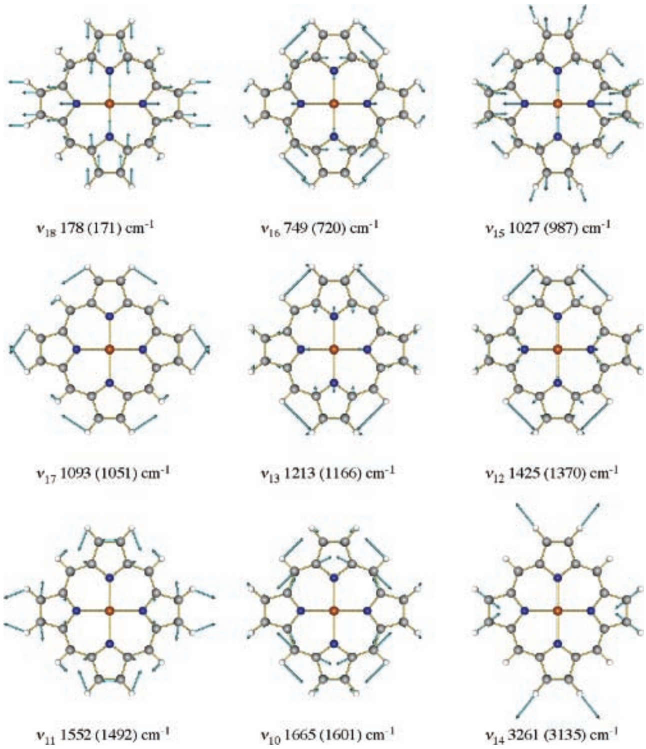

Figure 3. Computed vibrational eigenvectors of the B_{1g} modes for Zn porphyrin.

In this equation, $Q_{B1g,m}$ is the *m*th B_{1g} normal coordinate, and $q_{B1g,m}$ is the dimensionless normal coordinate.[26] Detailed procedures for the calculation of the coupling constant are described in previous papers.[27]

Results and Discussion

Vibronic Coupling for the B_{1g} Modes. The DFT B3LYP method is one of the most cost-effective and successful procedures for predicting vibrational frequencies of molecules.[28,29] The frequency scaling factor determined for the B3LYP method from a set of 122 molecules (1066 frequencies) is 0.9614,[29] which means that calculated vibrational frequencies can be used without scaling. Computed eigenvectors of the B_{1g} modes for Zn porphyrin are shown in Figure 3, in which scaled frequency values are shown in parentheses. It is useful to characterize these vibrational modes in detail before looking at computed vibronic coupling constants. The highest-frequency mode of ν_{14} is a C_β−H stretching mode, and the ν_{10} and ν_{11} modes are mainly due to C_α−C_m and C_β−C_β stretching, respectively. The ν_{12}, ν_{13}, and ν_{17} modes are assigned to vibrations that mainly involve C_β−H bending. The ν_{15} and ν_{16} modes are assigned to pyrrole-ring deformation modes, and the lowest-frequency mode of ν_{18} is due to Zn−N stretching. Calculated frequencies of the B_{1g} modes as well as metal−N bond distances for all the metalloporphyrins are listed in Table 2. As expected, only the ν_{18} modes are significantly dependent on the incorporated transition metals because they are a metal−N stretching mode, whereas the variation of the frequencies in the other modes is not so large.

TABLE 2: Metal−N Distances (in Units of Å) and Vibrational Frequencies (in Units of cm^{-1}) for the B_{1g} Modes of the Metalloporphyrins Calculated at the B3LYP/6-31G* Level of Theory[a]

mode	Cr	Mn	Fe	Co	Ni	Cu	Zn
M−N	2.042	2.083	1.989	1.976	1.957	2.007	2.043
ν_{18}	248 (238)	208 (200)	242 (233)	239 (230)	235 (226)	203 (195)	178 (171)
ν_{16}	749 (720)	747 (718)	744 (715)	748 (719)	748 (719)	747 (718)	749 (720)
ν_{15}	1035 (995)	1029 (989)	1018 (979)	1026 (986)	1027 (987)	1026 (986)	1027 (987)
ν_{17}	1093 (1051)	1091 (1049)	1094 (1052)	1096 (1054)	1097 (1055)	1095 (1053)	1093 (1051)
ν_{13}	1219 (1172)	1208 (1161)	1226 (1179)	1226 (1179)	1228 (1081)	1219 (1172)	1213 (1166)
ν_{12}	1427 (1372)	1423 (1368)	1427 (1372)	1432 (1377)	1433 (1378)	1430 (1375)	1425 (1370)
ν_{11}	1546 (1486)	1541 (1482)	1553 (1493)	1564 (1504)	1570 (1509)	1560 (1500)	1552 (1492)
ν_{10}	1654 (1590)	1634 (1571)	1681 (1616)	1701 (1635)	1715 (1649)	1688 (1623)	1665 (1601)
ν_{14}	3262 (3136)	3259 (3133)	3265 (3139)	3265 (3139)	3266 (3140)	3263 (3137)	3261 (3135)

[a] The values in parentheses are scaled by a factor of 0.9614.

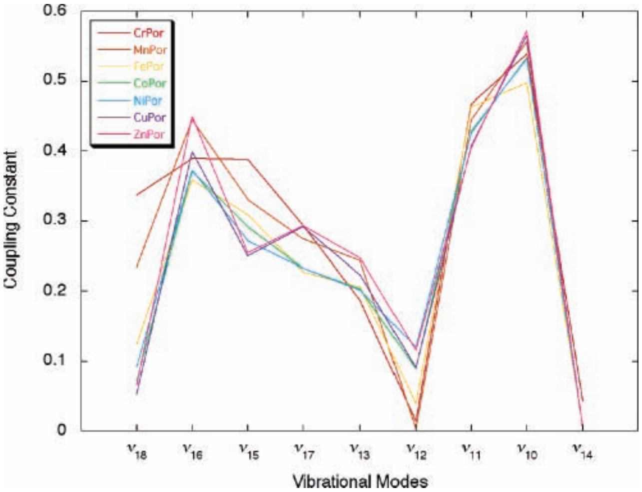

Figure 4. Dimensionless vibronic coupling constants for the B_{1g} modes of the metalloporphyrins.

Figure 4 presents calculated vibronic coupling constants for the B_{1g} modes of a series of metalloporphyrins. There is almost all no change for different metals except for the ν_{18} and ν_{15} modes, which have large vibration amplitudes on metal−N stretching. The result shows that the ν_{10} and ν_{11} modes, which are due to C_α−C_m and C_β−C_β stretching, respectively, have large coupling constants. The atomic displacements of these vibrational modes are large at the C_α, C_β, and C_m positions, where the e_g LUMOs have considerable orbital coefficients, and therefore the variation of these atomic positions results in a

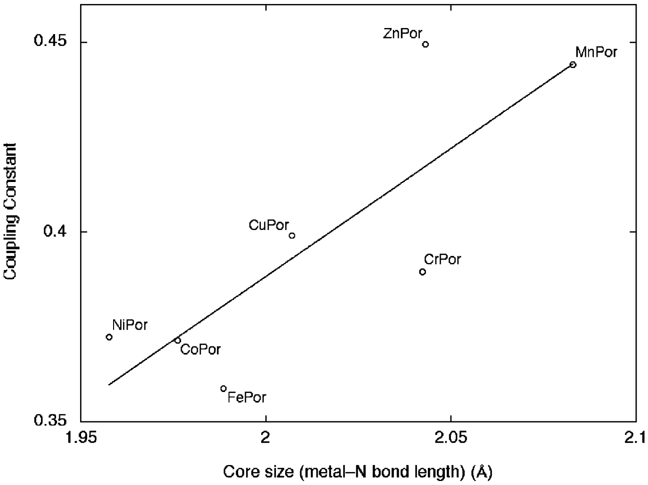

Figure 5. Vibronic coupling constants for the ν_{16} modes as a function of the core size of the metalloporphyrins.

significant interaction with the e_g LUMOs. One of the LUMOs is stabilized in energy and occupied by one electron while the other is destabilized and remains unoccupied. As a consequence, the total energy is decreased by the rectangular D_{2h} distortion along the ν_{10} and ν_{11} modes. This is a reasonable result from the viewpoint of orbital interactions. Spiro and co-workers[18d] reported from resonance Raman measurements and empirical normal-mode analyses that a rectangular B_{1g} distortion of the porphyrin ring should occur in the π-anion radical of vanadyltetraphenylporphyrin. In fact, the observed B_{1g} modes of $C_\alpha-C_m$ and $C_\beta-C_\beta$ stretching are significantly shifted upon one-electron reduction. In a similar sense the ν_{16} modes give large coupling constants because they have large amplitudes of vibration vector at the C_m positions. Although JT distortion is derived from the sum of the contributions of each vibrational mode, these three vibrational modes will play a central role in the geometrical change from D_{4h} to D_{2h}. On the other hand, since the ν_{14} modes are a C−H stretching mode, and in these vibrational modes the atomic displacements are large at the H atoms attached to the C_β positions. As a result, the ν_{14} modes do not have large coupling constants. This C−H stretching mode will play a minor role.

The incorporation of transition metals with different occupancies of d-orbitals between 4 and 10 reasonably changes the core size of the porphyrin ring, represented by the metal−N bond distances.[11] The core size increases in general with an increase in the number of d-electrons and the spin multiplicity. The largest core size is observed for the $^6A_{2g}$ state of Mn porphyrin, whereas the smallest core size is observed for the $^1A_{1g}$ state of Ni porphyrin. The second largest core size is found for the $^5B_{2g}$ state of Cr porphyrin and the $^1A_{1g}$ state of Zn porphyrin. To look at the core size dependence on the vibronic coupling constant, we plotted in Figure 5 computed coupling constants for the ν_{16} modes as a function of core size. It is found that the coupling constants increase with an increase in core size. The ν_{16} modes have large amplitudes of vibration vector at the C_m and N positions; in these pyrrole-ring deformation modes the $C_\alpha-C_m$ bonds are significantly changed in length while the $C_\beta-C_\beta$ bonds remain unchanged. The core size expansion is mainly associated with the increase of the $C_\alpha-C_m$ bond length and a change of the $C_\alpha-C_m-C_\alpha$ angle.[30] This correlation reflects the fact that the ν_{16} modes have significant contribution from $C_\alpha-C_m$ stretching and $C_\alpha-C_m-C_\alpha$ bending. Since the ν_{15} and ν_{18} modes have large vibration amplitudes on metal−N stretching, as mentioned earlier in this paper, it is interesting to look at how the coupling constants for these modes change as a function of core size. As shown in Figures S1 and S2 of Supporting Information, computed coupling constants for the ν_{15} and ν_{18} modes also tend to increase with core size.

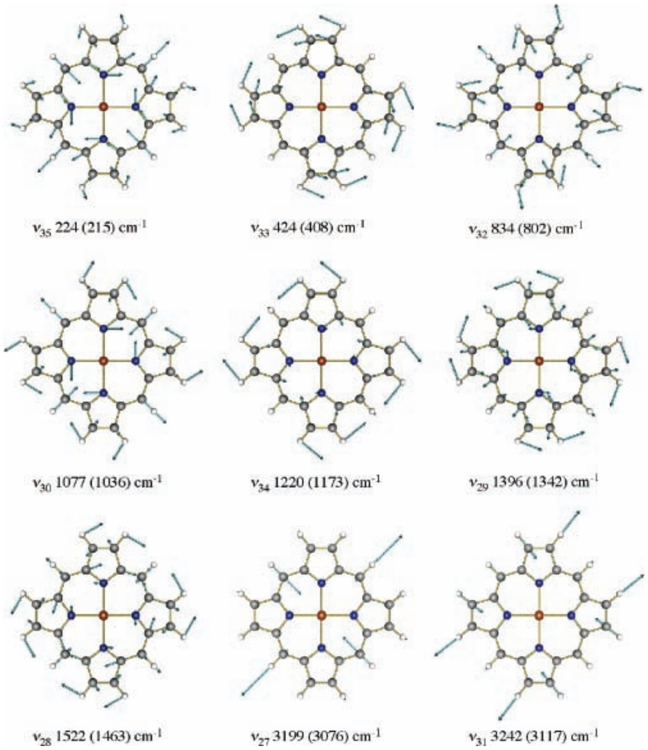
ν_{35} 224 (215) cm^{-1} ν_{33} 424 (408) cm^{-1} ν_{32} 834 (802) cm^{-1}
ν_{30} 1077 (1036) cm^{-1} ν_{34} 1220 (1173) cm^{-1} ν_{29} 1396 (1342) cm^{-1}
ν_{28} 1522 (1463) cm^{-1} ν_{27} 3199 (3076) cm^{-1} ν_{31} 3242 (3117) cm^{-1}

Figure 6. Computed vibrational eigenvectors of the B_{2g} modes for Zn porphyrin.

Vibronic Coupling for the B_{2g} Modes. Computed B_{2g} modes for Zn porphyrin are shown in Figure 6. The highest-frequency mode of ν_{31} is a C_β−H stretching mode, and the ν_{27} mode is a C_m−H stretching mode. The ν_{28} mode is assigned mainly to $C_\alpha-C_m$ stretching. The ν_{29}, ν_{24}, and ν_{30} modes are mainly due to C_β−H bending slightly mixed with Zn−N bending. The ν_{32} and ν_{33} modes are assigned to ring-deformation modes, and the lowest-frequency mode of ν_{35} is mainly due to Zn−N bending. Admixture of Zn−N bending is characteristic of the B_{2g} modes, whereas that of Zn−N stretching is characteristic of the B_{1g} modes. Table 3 lists calculated frequencies of the B_{2g} modes for all the metalloporphyrins. These vibrational modes are independent of the incorporated transition metals in frequency except for the ν_{18} modes.

Figure 7 shows calculated vibronic coupling constants for the B_{2g} modes of the metalloporphyrins. The ν_{29} modes have large coupling constants because they have large vibration amplitudes at the C_α, C_β, and N positions, in which the e_g LUMOs have considerable orbital amplitudes at the same time. However, the coupling constants for the B_{2g} modes are small in general compared to those for the B_{1g} modes because the B_{2g} modes include the metal−N bending character that would weakly couple with the ^2E_g state of the π-anion radicals. This computational result tells us that the rectangular D_{2h} distortion along the B_{1g} modes should occur rather than the diamond-like D_{2h} distortion along the B_{2g} modes in the JT effect of the π-anion radicals of the metalloporphyrins.

Conclusions

In this manuscript we have reported fundamental aspects on the JT effect in the π-anion radicals of the metalloporphyrins that incorporate Cr, Mn, Fe, Co, Ni, Cu, and Zn in terms of vibronic coupling constants. The original D_{4h} structure is

TABLE 3: Metal−N Distances (in Units of Å) and Vibrational Frequencies (in Units of cm^{-1}) for the B_{2g} Modes of the Metalloporphyrins Calculated at the B3LYP/6-31G* Level of Theory[a]

mode	Cr	Mn	Fe	Co	Ni	Cu	Zn
M−N	2.042	2.083	1.989	1.976	1.957	2.007	2.043
ν_{35}	207	194	227	235	240	227	224
	(199)	(187)	(218)	(226)	(231)	(218)	(215)
ν_{33}	425	418	434	435	438	430	424
	(409)	(402)	(417)	(418)	(421)	(413)	(408)
ν_{32}	834	832	833	833	833	833	834
	(802)	(800)	(801)	(801)	(801)	(801)	(802)
ν_{30}	1069	1066	1075	1082	1085	1081	1077
	(1028)	(1025)	(1034)	(1040)	(1043)	(1039)	(1035)
ν_{34}	1223	1214	1229	1230	1232	1226	1220
	(1176)	(1167)	(1182)	(1183)	(1184)	(1179)	(1173)
ν_{29}	1394	1390	1396	1402	1403	1399	1396
	(1340)	(1336)	(1342)	(1348)	(1349)	(1345)	(1342)
ν_{28}	1520	1504	1541	1548	1556	1536	1522
	(1461)	(1446)	(1482)	(1488)	(1496)	(1477)	(1463)
ν_{27}	3203	3194	3210	3210	3215	3206	3199
	(3079)	(3070)	(3086)	(3086)	(3090)	(3082)	(3076)
ν_{31}	3243	3240	3246	3245	3247	3244	3242
	(3118)	(3115)	(3121)	(3120)	(3122)	(3119)	(3117)

[a] The values in parentheses are scaled by a factor of 0.9614.

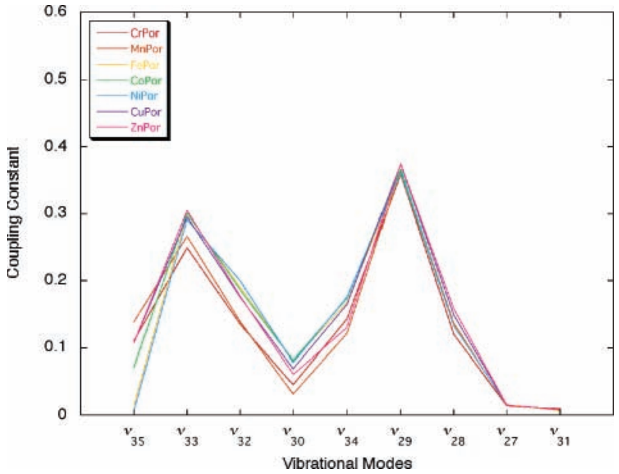

Figure 7. Dimensionless vibronic coupling constants for the B_{2g} modes of the metalloporphyrins.

distorted to a rectangular D_{2h} one by the B_{1g} modes of vibration. Although the B_{2g} modes can also lead to a diamond-like D_{2h} distortion, coupling constant calculations have shown that they would not play a major role in the JT distortion. Therefore, the B_{1g} modes are JT active in the π-anion radicals of the metalloporphyrins. Since there are more than one set of JT active B_{1g} modes, the JT effect in the π-anion radicals can be derived from the sum of the contributions of each B_{1g} vibrational mode. However, specific modes of vibration play a principal role in the structural change from D_{4h} to D_{2h} symmetry. The two B_{1g} modes of ν_{10} and ν_{11} that are assigned to C_α−C_m and C_β−C_β stretching modes, respectively, have very large vibronic coupling constants. Since the atomic displacements of these modes are large at the C_α, C_β, and C_m positions, where the e_g LUMOs have considerable orbital coefficients, the variation of these atomic positions results in a significant interaction with the e_g LUMOs. These C−C stretching modes will play a central role in the JT effect of the π-anion radicals of the metalloporphyrins. Computed vibronic coupling constants are similar for different metal ions, which demonstrates that the π-electron system of the porphyrin ring is not significantly perturbed by the central metal ions. The present vibronic interaction study is consistent with the Raman spectroscopic studies.[17,18]

Acknowledgment. K.Y. acknowledges Grants-in-Aid (Nos. 18350088, 18GS02070005, and 18066013) for Scientific Research from the Japan Society for the Promotion of Science (JSPS), the Ministry of Culture, Sports, Science and Technology of Japan (MEXT), the Nanotechnology Support Project of MEXT, the Joint Project of Chemical Synthesis Core Research Institutions of MEXT, and CREST of Japan Science and Technology Cooperation for their support of this work. T.K. acknowledges a Grant-in-Aid (No. 18750048) for Young Scientists B from JSPS. The sabbatical stay of P.M.K. at Kyushu University was supported by the Institute for Materials Chemistry and Engineering.

Supporting Information Available: Complete ref 23, one table of Cartesian coordinates for optimized structures of the metalloporphyrins, and two figures for computed coupling constants for the ν_{15} and ν_{18} modes as a function of core size. These materials are available free of charge via the Internet at http://pubs.acs.org.

References and Notes

(1) Dolphin, D., Ed. In *The Porphyrins*; Academic Press: New York, 1978; Vols. I−IV.

(2) Parson, W. W. In *Chlorophylls*; Scheer, H., Ed.; CRC Press: Boca Raton, FL, 1991; pp 1153−1180.

(3) Kadish, K. M., Smith, K. M., Guilard R., Eds. In *The Porphyrin Handbook*; Academic Press: San Diego, CA, 2000.

(4) Gouterman, M. In *The Porphyrins*; Dolphin, D., Ed.; Academic Press: New York, 1979; Vol. III, pp. 1−166.

(5) For example: (a) Englman, R. *The Jahn−Teller Effect in Molecules and Crystals*; Wiley: London, 1972. (b) Fischer, G. *Vibronic Coupling: The Interaction Between the Electronic and Nuclear Motions*; Academic Press: London, 1984. (c) Bersuker, I. B. *The Jahn−Teller Effect and Vibronic Interactions in Modern Chemistry*; Plenum Press: New York, 1984. (d) Bersuker, I. B.; Polinger, V. Z. *Vibronic Interactions in Molecules and Crystals*, Springer-Verlag: Berlin, 1989.

(6) (a) Bersuker, I. B.; Stavrov, S. S. *Coord. Chem. Rev.* **1988**, *88*, 1. (b) Bersuker, I. B.; Stavrov, S. S. *Chem. Phys.* **1981**, *54*, 331. (c) Bersuker, I. B.; Stavrov, S. S.; Vekhter, B. G. *Chem. Phys.* **1982**, *69*, 165. (d) Bersuker, I. B.; Stavrov, S. S. *Inorg. Chim. Acta* **1983**, *79*, 177. (e) Stavrov, S. S.; Bersuker, I. B. *Inorg. Chim. Acta* **1986**, *79*, 176.

(7) Hoffman, B. M.; Ratner, M. A. *Mol. Phys.* **1978**, *35*, 901.

(8) Prendergast, K.; Spiro, T. G. *J. Phys. Chem.* **1991**, *95*, 9728.

(9) Vangberg, T.; Lie, R.; Ghosh, A. *J. Am. Chem. Soc.* **2002**, *124*, 8122.

(10) Xu, L.-C.; Li, Z.-Y.; He, T.-J.; Liu, F.-C.; Chen, D.-M. *Chem. Phys.* **2004**, *305*, 165.

(11) Hirao, H.; Shaik, S.; Kozlowski, P. M. *J. Phys. Chem. A* **2006**, *110*, 6091.

(12) (a) Closs, G. L.; Closs, L. E. *J. Am. Chem. Soc.* **1963**, *85*, 818. (b) Dodd, J. W.; Hush, N. S. *J. Chem. Soc.* **1964**, 4607. (c) Felton, R. H.; Linschitz, H. *J. Am. Chem. Soc.* **1966**, *88*, 1113.(d) Hush, N. S.; Rowlands, J. R. *J. Am. Chem. Soc.* **1967**, *89*, 2976.(e) Peychal-Heiling, G.; Wilson, G. S. *Anal. Chem.* **1971**, *43*, 550. (f) Kholmogorov, V. E.; Maslov, V. G. *Opt. Spectrosc.* **1971**, 195. (g) Sutherland, J. C.; Axelrod, D.; Klein, M. P. *J. Chem. Phys.* **1972**, *54*, 2888. (h) Lexa, D.; Reix, J. *Chim. Phys. Physicochim. Biol.* **1974**, *71*, 517. (i) Donhoe, R. J.; Atamian, M.; Bocian, D. F. *J. Am. Chem. Soc.* **1987**, *109*, 5593. (j) Renner, M. W.; Fujita, E.; Fujita, I.; Procyk, A. D.; Bocian, D. F.; Fajer, J. *J. Phys. Chem.* **1992**, *96*, 9597. (k) Seth, J.; Bocian, D. F. *J. Am. Chem. Soc.* **1994**, *116*, 143.

(13) (a) Spiro, T. G.; Streaks, T. C. *J. Am. Chem. Soc.* **1974**, *96*, 338. (b) Rakhit, G.; Spiro, T. G.; Uyeda, M. *Biochem. Biophys. Res. Commun.* **1976**, *71*, 803. (c) Spiro, T. G. In *Iron Porphyrins*; Lever, A. B. P., Gray, H. B. Eds.; Addison-Wesley: Reading, MA, 1983; pp 85−159. (d) Czernuszewicz, R. S.; Macor, K. A.; Li, X.-Y.; Kincaid, J. R.; Spiro, T. G. *J. Am. Chem. Soc.* **1989**, *111*, 3860.

(14) (a) Kitagawa, T.; Iizuka, T.; Ikeda-Saito, M.; Kyogoku, Y. *Chem. Lett.* **1975**, 849. (b) Kitagawa, T.; Kyogoku, Y.; Iizuka, T.; Ikeda-Saito, M. *J. Am. Chem. Soc.* **1976**, *98*, 5169. (c) Kitagawa, T.; Teraoka, J. In *The Biological Chemistry of Iron*; Dunford, H. B., Dolphin, D., Raymond, K. N., Sieker, L., Eds.; D. Reidel: Dortrecht, The Netherlands, 1982; p 375.

(15) (a) Felton, R. H.; Romans, A. Y.; Yu, N.-T.; Schonbaum, G. R. *Biochem. Biophys. Acta* **1976**, *434*, 82. (b) Felton, R. H.; Yu, N.-T. In *The Porphyrins*; Dolphin, D., Ed.; Academic Press: New York, 1978; Vol. III, pp 347−393.

(16) (a) Yamaguchi, H.; Nakao, M.; Itoh, K. *Chem. Lett.* **1982**, 1397. (b) Yamaguchi, H.; Soeta, A.; Toeda, H.; Itoh, K. *J. Electroanal. Chem.* **1983**, *159*, 347.

(17) (a) Atamian, M.; Donohoe, R. J.; Lindsey, J. S.; Bocian, D. F. *J. Phys. Chem.* **1989**, *93*, 2236. (b) Perng, J.-H.; Bocian, D. F. *J. Phys. Chem.* **1992**, *96*, 4804. (c) Perng, J.-H.; Bocian, D. F. *J. Phys. Chem.* **1992**, *96*, 10234. (d) Procyk, A. D.; Stolzenberg, A. M.; Bocian, D. F. *Inorg. Chem.* **1993**, *32*, 627.

(18) (a) Reed, R. A.; Purrello, R.; Prendergast, K.; Spiro, T. G. *J. Phys. Chem.* **1991**, *95*, 9720. (b) Hu, S.; Lin, C.-Y.; Blackwood, M. E., Jr.; Mukherjee, A.; Spiro, T. G. *J. Phys. Chem.* **1995**, *99*, 9694. (c) Lin, C.-Y.; Spiro, T. G. *Inorg. Chem.* **1996**, *35*, 5237. (d) Lin, C.-Y.; Spiro, T. G. *Inorg. Chem.* **1996**, *35*, 5237. (e) Blackwood, M. E.; Lin, C.-Y.; Cleary, S. R.; McGlashen, M. M.; Spiro, T. G. *J. Phys. Chem. A* **1997**, *101*, 255. (f) Lin, C.-Y.; Blackwood, M. E.; Kumble, R.; Hu, S.; Spiro. T. G. *J. Phys. Chem. B* **1997**, *101*, 2373. (g) Blackwood, M. E.; Spiro, T. G. *J. Phys. Chem. B* **1997**, *101*, 8363.

(19) (a) Becke, A. D. *Phys. Rev. A* **1988**, *38*, 3098. (b) Becke, A. D. *J. Chem. Phys.* **1993**, *98*, 5648.

(20) Lee, C.; Yang, W.; Parr, R. G. *Phys. Rev. B* **1988**, *37*, 785.

(21) Stephens, P. J.; Devlin, F. J.; Chabalowski, C. F.; Frisch, M. J. *J. Phys. Chem.* **1994**, *98*, 11623.

(22) (a) Ditchfield, R.; Hehre, W. J.; Pople, J. A. *J Chem. Phys.* **1971**, *54*, 724. (b) Hehre, W. J.; Ditchfield, R.; Pople, J. A. *J Chem. Phys.* **1972**, *56*, 2257. (c) Hariharan, P. C.; Pople, J. A. *Theoret. Chim. Acta.* **1973**, *28*, 213. (d) Rassolov, V. A.; Pople, J. A.; Ratner, M. A.; Windus, T. L. *J. Chem. Phys.* **1998**, *109*, 1223.

(23) Frisch, M. J. et al. *Gaussian 03*, revision C.02; Gaussian Inc.: Wallingford, CT, 2004.

(24) Kozlowski, P. M.; Rush, T. S.; Jarzecki, A. A.; Zgierski, M. Z.; Chase, B.; Piffat, C.; Ye, B.-H.; Li, X.-Y.; Pulay, P.; Spiro, T. G. *J. Phys. Chem. A* **1999**, *103*, 1357.

(25) Czernuszewicz, R. S.; Li, X.-Y.; Spiro, T. G. *J. Am. Chem. Soc.* **1989**, *111*, 7024.

(26) Conwell, E. M. *Phys. Rev. B* **1980**, *22*, 1761.

(27) (a) Yoshizawa, K.; Kato, T.; Yamabe, T. *J. Chem. Phys.* **1998**, *108*, 7637. (b) Yoshizawa, K.; Kato, T.; Yamabe, T. *J. Chem. Phys.* **1998**, *109*, 8514. (c) Yoshizawa, K.; Kato, T.; Tachibana, M.; Yamabe, T. *J. Phys. Chem. A* **1998**, *102*, 10113.

(28) Rauhut, G.; Pulay, P. *J. Phys. Chem.* **1995**, *99*, 3093.

(29) Scott, A. P.; Radom, L. *J. Phys. Chem.* **1996**, *100*, 16502.

(30) Prebdergast, K.; Spiro, T. G. *J. Am. Chem. Soc.* **1992**, *114*, 3793.